



Contents lists available at ScienceDirect

Physics Letters A

www.elsevier.com/locate/pla

Enhanced negative thermal expansion and optical absorption of $\text{In}_{0.6}(\text{HfMg})_{0.7}\text{Mo}_3\text{O}_{12}$ with oxygen vacancies

Yongguang Cheng^{a,b}, Yanchao Mao^a, Baohe Yuan^a, Xianghong Ge^a, Juan Guo^a, Mingju Chao^a, Erjun Liang^{a,*}^a School of Physical Science & Engineering and Key Laboratory of Materials Physics of Ministry of Education of China, Zhengzhou University, Zhengzhou, 450051, China^b College of Science, Center of Analysis and Testing of Henan Institute of Engineering, Zhengzhou 451191, China

ARTICLE INFO

Article history:

Received 2 December 2016

Received in revised form 12 April 2017

Accepted 2 May 2017

Available online xxxx

Communicated by M. Wu

Keywords:

Oxygen vacancies

Negative thermal expansion

Near-zero thermal expansion

Structure analysis

ABSTRACT

A negative thermal expansion (NTE) material $\text{In}_{0.6}(\text{HfMg})_{0.7}\text{Mo}_3\text{O}_{12}$ with oxygen vacancies was successfully synthesized through He atmosphere annealing. It was found that the introduction of oxygen vacancies enhanced the coefficient of NTE by about an order of magnitude larger. It can be attributed to the increased flexibility of the polyhedra in the framework structure. The introduction of oxygen vacancies also weakened the M=O bonds and obviously enhanced the optical absorption in the visible light region. This work provides a promising strategy to effectively improve the NTE and optical properties of traditional NTE materials by introducing oxygen vacancies.

© 2017 Elsevier B.V. All rights reserved.

1. Introduction

Negative thermal expansion (NTE) materials have attracted tremendous interests since the rediscovery of NTE properties in cubic ZrW_2O_8 [1]. It holds great potential applications in reducing thermal stress of mechanical and electrical devices [2–7]. Among a series of NTE materials, $\text{A}_2\text{M}_3\text{O}_{12}$ family has a framework structure with large chemical flexibility [8–15], where A is a transition metal or rare earth, and M is the W or Mo. The $\text{A}_2\text{M}_3\text{O}_{12}$ family has the orthorhombic or monoclinic symmetry at room temperature. Both the orthorhombic and monoclinic structures are composed of AO_6 octahedron and MO_4 tetrahedron [16,17]. It is worth to note that only the corner-sharing orthorhombic structure exhibits NTE properties. In the orthorhombic structure, the A–O–M linkages could result in the transverse thermal vibrations of the bridging oxygen, and also the librational or translational vibrations of the A and M atoms. Such vibrations induce the contract of the material with temperature increasing [14,18].

$\text{In}_2\text{Mo}_3\text{O}_{12}$ has a monoclinic structure at room temperatures, and it will transform to the orthorhombic structure above 616 K [19]. It exhibits thermal expansion in the monoclinic phase and

thermal contraction in the orthorhombic structure. $\text{HfMgMo}_3\text{O}_{12}$ was reported to have the low positive thermal expansion property [20]. $\text{In}(\text{HfMg})_{0.5}\text{Mo}_3\text{O}_{12}$ was found to be a near-zero thermal expansion material above 423 K after the monoclinic to orthorhombic phase transition occurred [21]. According to the previous report [22], it is predictable that the temperature of phase transition can be further reduced by increasing the ratio of the $(\text{HfMg})^{6+}$ cations.

In this paper, we fabricated the $\text{In}_{0.6}(\text{HfMg})_{0.7}\text{Mo}_3\text{O}_{12}$ NTE material with oxygen vacancies through He atmosphere annealing. It was found that the NTE and light absorption properties of the material were remarkably enhanced after introducing oxygen vacancies. The related mechanism was also discussed.

2. Experimental section

2.1. Synthesis of $\text{In}_{0.6}(\text{HfMg})_{0.7}\text{Mo}_3\text{O}_{12}$ bulk ceramic

The starting materials of In_2O_3 , HfO_2 , MgO and MoO_3 were mixed according to the molar ratio of $\text{In}_{0.6}(\text{HfMg})_{0.7}\text{Mo}_3\text{O}_{12}$. The mixtures were ground for 2 h followed by annealing at 1073 K for 5 h in air and cooled naturally to the room temperature. Then the calcined powders were uniaxially cold pressed at 300 MPa into square pellets. The pellets were re-sintered at 973 K for 3 h in air. The samples were further annealed at 773 K for 5 min in He atmosphere to introduce oxygen vacancies.

* Corresponding author. Fax: +86 371 67766629.

E-mail address: ejliang@zzu.edu.cn (E. Liang).

<http://dx.doi.org/10.1016/j.physleta.2017.05.002>

0375-9601/© 2017 Elsevier B.V. All rights reserved.

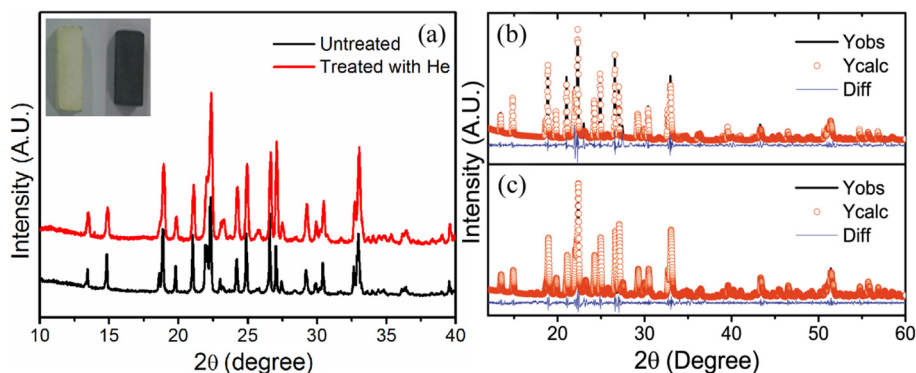


Fig. 1. (a) XRD patterns of $\text{In}_{0.6}(\text{HfMg})_{0.7}\text{Mo}_3\text{O}_{12}$ at room temperature: The black line is the XRD pattern of the untreated sample, the red line is the XRD pattern of the sample treated with He. The insert is the photo of the samples untreated (white) and the sample treated with He (black). (b) and (c) are the results of Le Bail fittings of the XRD data using the space group P21/a for $\text{In}_{0.6}(\text{HfMg})_{0.7}\text{Mo}_3\text{O}_{12}$ and $\text{In}_{0.6}(\text{HfMg})_{0.7}\text{Mo}_3\text{O}_{12}\text{-He}$, respectively. The measured pattern is in black solid line, the fitted pattern is red circle, and the difference plot is blue. (For interpretation of the references to color in this figure legend, the reader is referred to the web version of this article.)

Table 1
Lattice constants of sample treated and untreated with He.

Lattice constants	$\text{In}_{0.6}(\text{HfMg})_{0.7}\text{Mo}_3\text{O}_{12}$	$\text{In}_{0.6}(\text{HfMg})_{0.7}\text{Mo}_3\text{O}_{12}\text{-He}$
a (Å)	16.2100(6)	16.2094(7)
b (Å)	9.5571(4)	9.5575(5)
c (Å)	18.8755(7)	18.8757(2)
β (°)	125.402(7)	125.400(2)
Unit cell volume (Å ³)	2383.535(7)	2383.664(1)

2.2. Characterization

X-ray diffraction (XRD) measurements were carried out with a Bruker D8 Advance X-ray diffractometer (Cu $K\alpha$ radiation, $\lambda = 1.5406 \text{ \AA}$) with an mri MTC-furnace A2FA5 high-temperature attachment, the heating rate is 10 K min^{-1} and hold on two minutes at every target temperature. Raman spectra were recorded with a Renishaw inVia Raman spectrometer with 325 nm laser wavelength excitation and the wavenumber range is from 100 to 1200 cm^{-1} . The surface morphology and energy dispersive spectra (EDS) were measured with a Quanta 250 scanning electron micrograph (SEM, USA FEI) with an AMETEK EDAX APOLLO XP energy dispersive spectrometer. The absorption spectra were carried out with a SHIMADZU UV3600 UV-Vis-IR spectrophotometer, the wavelength range is from 200 to 800 nm. The linear coefficients of thermal expansion (CTE) were measured with a dilatometer (Linseis DIL L76) with the heating rate is 5 K min^{-1} .

3. Results and discussion

3.1. X-ray diffraction study

Fig. 1(a) shows the XRD patterns of $\text{In}_{0.6}(\text{HfMg})_{0.7}\text{Mo}_3\text{O}_{12}$ samples before and after annealing in He atmosphere (denoted as $\text{In}_{0.6}(\text{HfMg})_{0.7}\text{Mo}_3\text{O}_{12}\text{-He}$). Photographs of both samples are shown in the insert of Fig. 1(a). The color of the sample treated in He atmosphere was found to be changed from white to black. Nevertheless, the XRD patterns for both samples are very similar except some subtle changes in relative peak intensities. Figs. 1(b) and (c) exhibit the results of Le Bail fittings of the XRD data using the space group P21/a for $\text{In}_{0.6}(\text{HfMg})_{0.7}\text{Mo}_3\text{O}_{12}$ and $\text{In}_{0.6}(\text{HfMg})_{0.7}\text{Mo}_3\text{O}_{12}\text{-He}$, respectively. The both samples crystallized in a monoclinic structure with space group P21/a. The calculated lattice parameters of $\text{In}_{0.6}(\text{HfMg})_{0.7}\text{Mo}_3\text{O}_{12}$ are $a = 16.2100(6)$, $b = 9.5571(2)$, $c = 18.8755(0)$, $\beta = 125.402(7)$ and $V = 2383.535(7)$. The lattice parameters of $\text{In}_{0.6}(\text{HfMg})_{0.7}\text{Mo}_3\text{O}_{12}\text{-He}$ are $a = 16.2094(7)$, $b = 9.5575(5)$, $c = 18.8757(7)$, $\beta = 125.400(2)$ and $V = 2383.664(1)$. Table 1 lists the lattice constants

of sample treated and untreated with He. The lattice parameters were increased after annealing in He atmosphere.

3.2. Energy dispersive spectrometer analysis

The EDS measurements were also carried out for the both samples as shown in Fig. 2. The EDS results of $\text{In}_{0.6}(\text{HfMg})_{0.7}\text{Mo}_3\text{O}_{12}$ and $\text{In}_{0.6}(\text{HfMg})_{0.7}\text{Mo}_3\text{O}_{12}\text{-He}$ obtained from the areas indicated by the squares in the corresponding SEM images. The elements In, Hf, Mg, Mo and O are all detected in the EDS spectrum for the $\text{In}_{0.6}(\text{HfMg})_{0.7}\text{Mo}_3\text{O}_{12}$ and $\text{In}_{0.6}(\text{HfMg})_{0.7}\text{Mo}_3\text{O}_{12}\text{-He}$.

3.3. Thermal expansion study

In order to investigate the effects of oxygen vacancies on the thermal expansion property, we measured the relative length change of $\text{In}_{0.6}(\text{HfMg})_{0.7}\text{Mo}_3\text{O}_{12}$ and $\text{In}_{0.6}(\text{HfMg})_{0.7}\text{Mo}_3\text{O}_{12}\text{-He}$. Above phase transition temperature of 358 K, the $\text{In}_{0.6}(\text{HfMg})_{0.7}\text{Mo}_3\text{O}_{12}$ exhibited a near zero thermal expansion property with the linear CTE of $\alpha_1 = -4.05 \times 10^{-7} \text{ K}^{-1}$ as shown in Fig. 3(a). The phase transition temperature was lowered by about 70 K with respect to that of $\text{In}(\text{HfMg})_{0.5}\text{Mo}_3\text{O}_{12}$ [21]. As to the $\text{In}_{0.6}(\text{HfMg})_{0.7}\text{Mo}_3\text{O}_{12}\text{-He}$, the phase transition temperature of $\text{In}_{0.6}(\text{HfMg})_{0.7}\text{Mo}_3\text{O}_{12}$ didn't changed after annealing in He atmosphere. Nevertheless, the relative length and linear NTE of the sample in the orthorhombic phase were enhanced according to the increased and more negative slope of the solid curve. The extrinsic linear NTE for $\text{In}_{0.6}(\text{HfMg})_{0.7}\text{Mo}_3\text{O}_{12}\text{-He}$ was calculated to be about $\alpha_2 = -2.11 \times 10^{-6} \text{ K}^{-1}$ which is about one order of magnitude larger than that of the $\text{In}_{0.6}(\text{HfMg})_{0.7}\text{Mo}_3\text{O}_{12}$.

We further measured the XRD patterns at different temperature and calculated the lattice parameters of each temperature for both samples by Le Bail refinement. Table 2 lists the lattice constants of orthorhombic space group at different temperature of sample treated and untreated with He atmosphere. The cell volume was increased at the same temperature compared with the cell volumes of the sample untreated with He. The intrinsic axial CTEs for the a-, b- and c-axis and linear CTEs were calculated and shown in the Table 3. It is shown that the intrinsic coefficients of NTE were enhanced for $\text{In}_{0.6}(\text{HfMg})_{0.7}\text{Mo}_3\text{O}_{12}\text{-He}$ compared to the $\text{In}_{0.6}(\text{HfMg})_{0.7}\text{Mo}_3\text{O}_{12}$. The intrinsic linear CTE of $\text{In}_{0.6}(\text{HfMg})_{0.7}\text{Mo}_3\text{O}_{12}\text{-He}$ was enhanced from $-4.7 \times 10^{-7} \text{ K}^{-1}$ to $-1.5 \times 10^{-6} \text{ K}^{-1}$. Fig. 3(b) shows the formula unit cell volume changed with temperature increasing of the both samples. The formula unit cell volumes exhibited similar behavior with temperature as the relative length changed. These results are consistent with the relative length change results.

Download English Version:

<https://daneshyari.com/en/article/5496291>

Download Persian Version:

<https://daneshyari.com/article/5496291>

[Daneshyari.com](https://daneshyari.com)